1 kV 150 A Bidirectional Isolated DC/DC Converter With Full Range ZVS For Charger Application

Rajendra Prasad Kandula
Oak Ridge National Laboratory
Knoxville, USA
kandular@ornl.gov

Rafal Wojda
Oak Ridge National Laboratory
Knoxville, USA
wojdarp@ornl.gov

Jonathan Harter
Oak Ridge National Laboratory
Knoxville, USA
harterjj@ornl.gov

Christian Boone
Oak Ridge National Laboratory
Knoxville, USA
boonecl@ornl.gov

***Abstract*— This paper focusses on the development of a bidirectional DC/DC converter based on dual active bridge (DAB) converter for 1 kV class fast charger applications. A novel modulation technique is proposed to achieve zero voltage switching across the entire operating range of a vehicle battery system. The topology includes a tap changer to support multiple class of vehicles. The full range ZVS operation will allow high efficiency operation even at light load, reduced *dv/dt* to improve transformer insulation lifetime and mitigate EMI impact. A 1 kV class, 150 A prototype was developed to validate the proposed concepts.**

Keywords—Isolated DC/DC converter, Dual active bridge, zero voltage switching, fast charger, bi-directional DC/DC converter.

I. INTRODUCTION

Fast chargers are required to have a wide voltage range to be compatible with both 400 V and 800 V class vehicles. A typical 800 V class vehicle may have a fast-charging range of 580 – 760 V while a 400 V class may have a fast-charging range of 290 – 380 V [1]. Electric semi-trucks with battery capacity in the range of 400-1000 kWh [11], will need MW class charging, which will need modules > 100 kW to reduce complexity. In addition, to be compatible with new vehicle to everything (V2X) requirements [2], chargers are expected to be bidirectional capable and have galvanic isolation to ensure user safety [3]. There are multiple architectures to implement fast chargers [4]. The two-stage architecture, which includes a common AC/DC converter and multiple isolated DC/DC converters, is preferred as it reduces the AC/DC converter rating considering the load diversity [4].

With the reducing cost of Silicon Carbide (SiC) devices [5], the next generation chargers are expected to use SiC based converters, at least for the DC/DC stage. With SiC, the converter can be operated at higher frequencies and thereby reduce the size of the isolation transformer. However, with SiC, it is desirable to maintain zero voltage switching (ZVS) to achieve high efficiency and more importantly control the *dv/dt* to protect the transformer insulation from degradation [6,10] and reduce EMI. In summary, the requirements for next generation fast chargers (DC/DC stage) include wide operating range (250-920 V), high power modules (>100 kW), galvanic isolation, bi-directionality and ZVS across the wide operating range.

Resonant based converters and DAB based converters are the two common ways to implement an isolated DC/DC converter. Most of the commercial fast chargers are based on LLC type resonant converter, which is not suitable for bidirectional operation. To achieve bidirectional operation with a resonant converter, CLLC converter was proposed. The CLLC converter has controllability and ZVS issues especially when required to operate across a wide operating range [4]. In case of DAB, the controllability is relatively easier compared to CLLC, but it retains the same ZVS problem when required to operate across a wide operating range.

Several modulation techniques have been proposed to improve the soft switching range of the DAB, with double phase shift (DPS) and triple phase shift (TPS) being the most common. Basic DPS modulation cannot achieve full range ZVS. The use of magnetizing current to achieve full range ZVS, while using DPS, is proposed in [7]. However, it requires relatively low magnetizing inductance. The design of DAB transformer with low magnetizing inductance makes it susceptible to saturation caused by DC offset during transients, dead time, PWM delays and others. TPS for full load range ZVS has been presented in [8,9]. However, here a factor of two is assumed between input and output voltage and the scheme may not be applicable where the variation is much smaller as in the case of charger.

In this paper, the development of a bidirectional DC/DC converter based on DAB for 1 kV class fast charger applications is presented. In section II, the converter architecture is presented. In Section III, constraints of standard modulation technique are presented. In Section IV, a novel modulation technique is proposed to achieve ZVS across the entire operating range of the converter. In Section V, the control architecture is presented, while in VI, the design of a 1 kV class 150 A converter prototype and the experimental results to demonstrate the proposed technique are presented. The conclusions regarding the performance and feasibility of the proposed converter and control approach are presented in Section VII.

II. PROPOSED DC/DC CHARGER CONFIGURATION

A. Architecture

The schematic of the proposed implementation of isolated DC/DC converter is shown in Fig. 1. The implementation is based on DAB except for the addition of taps on the transformer secondary. The taps are selected to choose between a 400 V class and an 800 V class vehicle. The taps are changed before the vehicle power contacts are closed and hence do not impact the

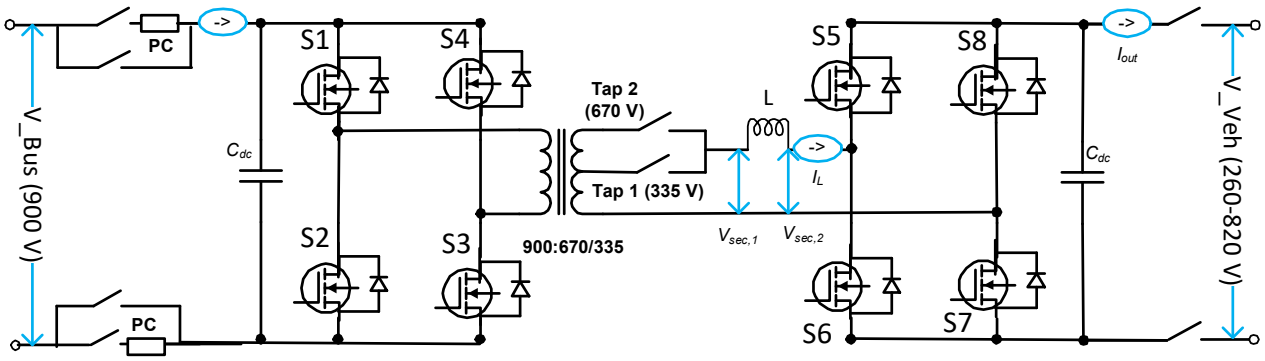

Fig. 1. Schematic of proposed implementation of isolated DC/DC converter.

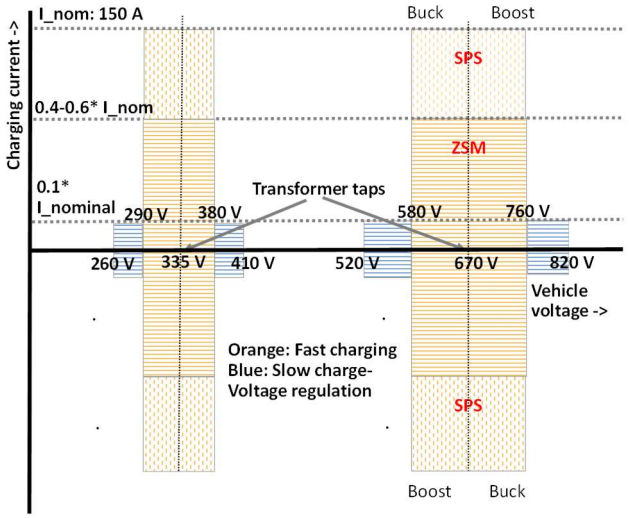

Fig. 2. ZVS range of the proposed DC/DC converter based on DAB.

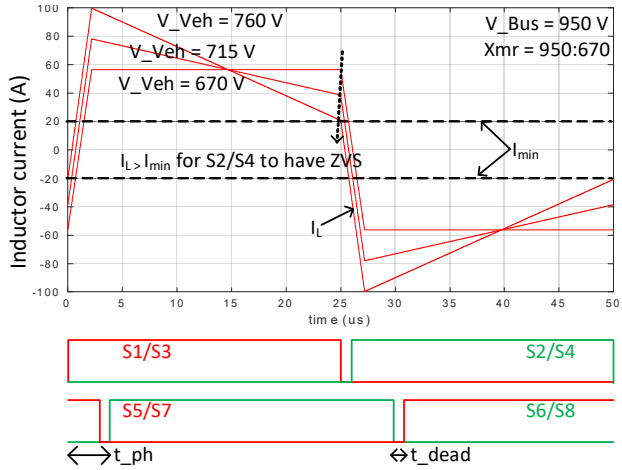

Fig. 3 Single Phase Shift (SPS) modulation in boost mode – variation in inductor current as V_Veh varies at constant phase shift.

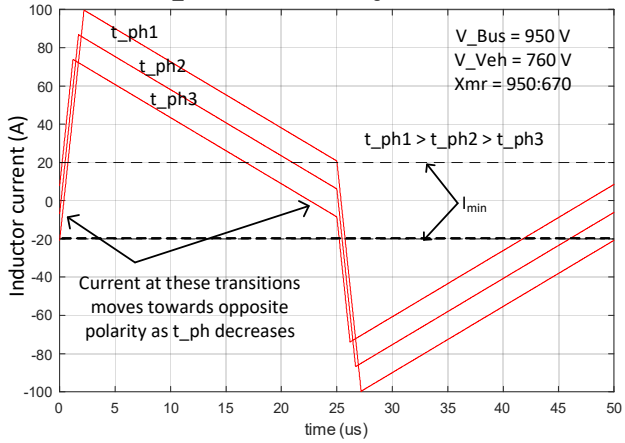

Fig. 4. SPS modulation in boost mode – variation in I_L with phase shift.

dynamic operation of the converter. An 800 V class vehicle has a fast-charging range of 580 – 760 V [1]. The first tap is selected at the mid point of this range at 670 V. This ensures the DAB must handle a limited variation of +/- 15%. Above 760 V, the vehicle will be in voltage regulation mode or will be charged at lower currents. Similarly for the 400 V class vehicle, the tap is chosen to be 335 V, positioned midway between the fast-charging range of 290-380 V. The targeted ZVS operating range of the converter is shown in Fig. 2. Standard phase shift (SPS) modulation technique will be used at higher currents (0.6-1.0x rated current), while zero state modualtion (ZSM) technique is proposed to be used at lower techniques. The split modulation scheme allows high efficiency and ZVS across the entire load range by taking advantage of the merits of each technique.

III. Standard DAB Modulation Constraints

The standard single-phase shift (SPS) modulation for the DAB in boost mode is shown in Fig. 3. SPS is optimal in terms of efficiency, however, ZVS region is limited. A switch will have ZVS if the current is flowing in the corresponding free-wheeling diode (FWD) at turn-on. For ZVS turn-on of $S2/S4$, the inductor current, I_L, needs to be positive at the instant of switching. Considering non-idealities such as dead time and device drain-source capacitances, I_L should be higher than a minimum value, I_{min}, to ensure ZVS. As shown in Fig. 3, as the vehicle voltage, V_veh, increases, I_L at the turn-on instant of $S2/S4$ tends to become less than I_{min} and hence lose ZVS. The taps selected in the previous section limits the V_veh variation to +/- 15% and helps in achieving ZVS for both 400 V and 800 V class vehicles at least at higher currents. However, as shown in Fig. 4, if the phase shift, t_{ph} is reduced to lower the current, I_L goes below I_{min} and switch $S2/S4$ again tends to lose ZVS. Similar arguments can be made for other switches and buck mode of operation.

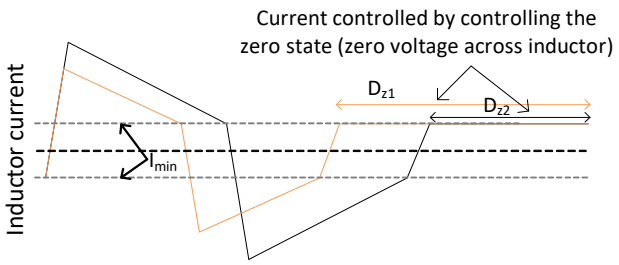

Fig. 5. Conceptual plot of propsoed zero state modulation (ZSM) scheme for lower currents – phase is kept constant and duty is varied.

IV. Proposed Zero State Modulation (ZSM)

This paper proposes modified modulation for lower currents and the basic idea is shown in Fig. 5. In SPS, the phase shift is varied to control the current, and the duty cycle is kept fixed at a maximum value (50%). In the proposed technique, phase is kept constant and duty cycle is varied to control the current. This method ensures that I_L at all transitions is higher than I_{min}, to achieve ZVS for all the switches even at near zero current. When the duty cycle is reduced below maximum, zero state (zero voltage across the phase inductor) is added for the remaining part of the switching cycle where no energy is exchanged between the two buses. Effectively, zero state controls current, hence this method is termed as zero state modulation (ZSM). The detailed switching scheme of the ZSM technique for boost mode is shown in Fig. 6. The inductor volt-secs are balanced over two switching cycles. Initially, the inductor current is negative but in a zero state. The first cycle starts with a positive current pulse and is followed by a negative current pulse and a zero state with positive I_L. The second cycle starts with a negative current pulse followed by a positive pulse and a zero state with negative I_L and the cycle repeats. The timings t_1, t_3, t_5 and t_z and the duty cycle D are varied to control the current while achieving ZVS and are obtained using the converter model. The timings t_1, t_3, t_5 are similar to the phase shifts in TPS method. Two different approaches, based on when the timings are derived, are proposed to implement ZSM and are explained here.

A. Optimal ZSM control

In the optimal ZSM control method, the timings t_1, t_3, t_5 and t_z are derived to ensure ZVS and to minimize the RMS current. This will happen when the source bridge current transitions are at $|I_{min}|$ in the case of boost mode and the load bridge transitions are at $|I_{min}|$ in case of buck mode. The timings t_1, t_3, t_5 and t_z are a function of duty cycle D, the smallest current to ensure ZVS I_{min}, phase inductor L_{ph}, voltages V_veh, and V_bus. In the optimal method, these timings are derived online during each switching cycle. The voltages are measured, $|I_{min}|$ is predetermined, L_{ph} is obtained from the converter and D is obtained from the output of the current control loop. For the boost operation, the timings are derived using (1) to (6). The constraints are given in (7).

$$t_1 = \frac{(V_{veh}-V_{bus})DT_s}{V_{veh}} + \frac{2I_{min}L_{ph}}{V_{veh}} \quad (1)$$

$$t_2 = DT_s - t_1 \quad (2)$$

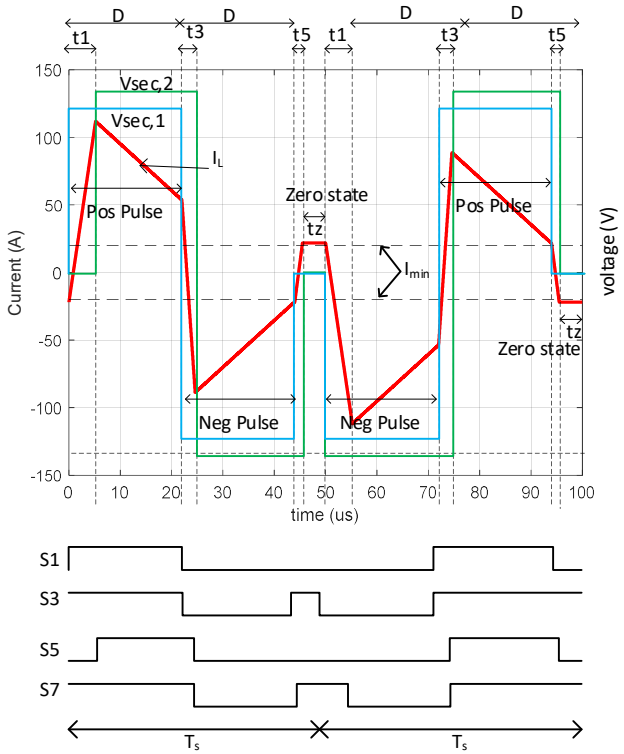

Fig. 6. Detailed switching scheme of the proposed ZSM technique.

$$t_3 = \frac{(V_{veh}-V_{bus})DT_s}{2V_{veh}} + \frac{I_{min}L_{ph}}{V_{veh}} \quad (3)$$

$$t_4 = DT_s - t_3 \quad (4)$$

$$t_5 = \frac{2I_{min}L_{ph}}{V_{veh}} \quad (5)$$

$$t_z = T_s(1-2D) - t_5 \quad (6)$$

$$D < 0.5(T_s - t_z - t_5)/T_s, V_{veh} \geq V_{bus} \quad (7)$$

For the buck operation the timings are derived using (8) to (13). The constraints are given (14).

$$t_1 = \frac{2I_{min}L_{ph}}{V_{bus}} \quad (8)$$

$$t_2 = DT_s - t_1 \quad (9)$$

$$t_3 = \frac{(V_{bus}-V_{veh})(DT_s-t_1)}{(V_{veh}+V_{bus})} + \frac{I_{min}L_{ph}}{(V_{veh}+V_{bus})} \quad (10)$$

$$t_4 = DT_s - t_3 \quad (11)$$

$$t_5 = \frac{(V_{bus}-V_{veh})t_4}{V_{veh}} + \frac{2I_{min}L_{ph}}{V_{veh}} \quad (12)$$

$$t_z = T_s(1-2D) - t_5 \quad (13)$$

$$D < 0.5(T_s - t_z - t_5)/T_s, V_{bus} \geq V_{veh} \quad (14)$$

The equations provided here assume the transformer turns ratio is 1:1. In case of non-unity turns-ratio, necessary conversion of current and voltages can be performed and the analysis can be done either on the primary or the secondary side.

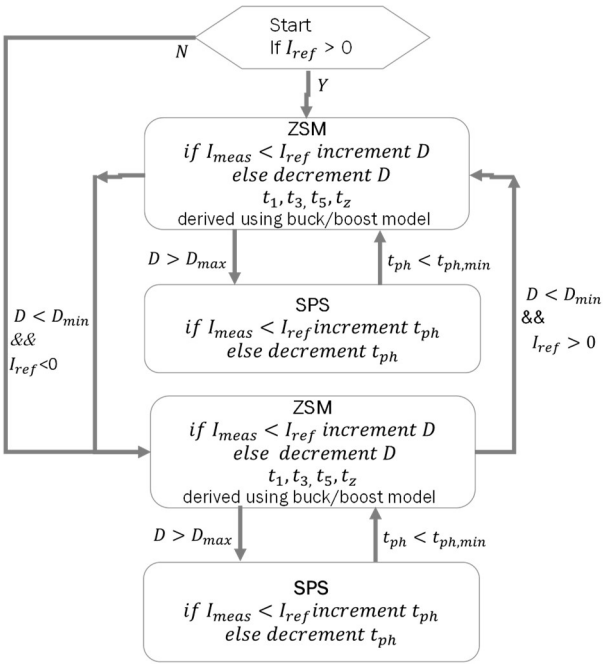

Fig. 7: State machine for implementation of proposed control.

For the reverse power flow operation, due to symmetry, the above analysis can be applied with minor changes. For example, the boost operation in forward power flow will become buck operation in reverse power flow. Hence the buck model given by (8)-(14) can be used with the V_{bus} and V_{veh} swapped. Simultaneously the pulses *S1/S3* must be swapped with *S5/S7*.

B. Simplified ZSM control

In the simplified ZSM control method, the timings t_1, t_3, t_5 and t_z are derived to ensure ZVS but the constraint to minimize the RMS current is removed. This will allow deriving the timings offline and no calculations are needed to be performed at every switching cycle. The offline calculations are performed for the worst case for ZVS conditions.

In the case of boost mode, the worst case is when $(V_{veh} - V_{bus})$ is at its maximum value. To derive the timings t_1, t_3, *and* t_5, the boost model (1)-(7) is used with values $max(V_{veh} - V_{bus})$, t_z=0, and D is $0.5(T_s - t_5)$.

Similarly, in case of buck mode, the worst case is when $(V_{bus} - V_{veh})$ is at its maximum value. To derive the timings t_1, t_3, *and* t_5, the buck model (8)-(14) is used but with values $max(V_{ve} - V_{bus})$, t_z=0, and D is $0.5(T_s - t_5)$.

As in the case of optimal control, reverse power flow involves simply swapping the bridges and timings.

C. Comparison with TPS

At a fundamental level, the proposed ZSM technique is similar to the triple phase shift (TPS) method proposed in [8]. Both the methods use the addition of zero state to control the current while ensuring ZVS. However the method in [8] applies only when the bus voltages significantly differ and has been demonstrated for only buck operation. The proposed method is universal in the sense that it is applicable for any bus voltages and for bi-directional power flow. In addition, the simplified ZSM method relies on a single variable D to control the current, improving the ease of implementation.

Fig. 8. Image of 1 kV class 150 A isolated DC/DC converter based on DAB.

V. Control Architecture

The operating region of the converter is shown in Fig. 2. At each tap, there are eight operating modes: Buck, boost, low current, and high current for the forward power flow and the same four for the reverse power flow. To ensure transient free operation between the modes, the state machine, shown in Fig. 7 is implemented. At the start, depending on the current reference, the control enters either the forward low-current mode or reverse low-current mode. Within the low-current mode, the current control is obtained by adjusting the duty cycle. The timings t_1, t_3, t_5 and t_z are derived using the buck or the boost model depending on the voltages. The control moves from low-current mode to high-current mode if D hits its upper limit of $D > 0.5(T_s - t_z - t_5)$. The control moves from forward/reverse low-current mode to reverse/forward low-current mode if the reference current I_{ref} becomes negative/positive and D hits its lower limit of zero. In the high current modes, the converter uses SPS modulation and the current control is achieved through adjusting the phase shift t_{ph}. The control moves from high-current mode to low-current mode if t_{ph} hits its lower limit of $t_{ph,min}$, which can be obtained by (3) for boost operation and by (10) for buck operation. $D > 0.5(T_s - t_z - t_5)$.

VI. Experimetnal Verification

A. 1 kV class 150 A Prototype

A 950 V, 150 A isolated DC/DC converter prototype, shown in Fig. 8, has been built. The main components used for the build are shown in TABLE I. The main bus is designed for a nominal voltage of 900 V and a peak of 950 V, while the vehicle bus is expected to vary from 250 V to 810 V. The converter is designed for 20 kHz operation.

The 20 kHz transformer is built with nanocrystalline core and Litz wire. The magnetizing inductance is chosen so that the magnetizing current is <10% of the transformer load current. The transformer is designed with 13/10 ratio. The transformer

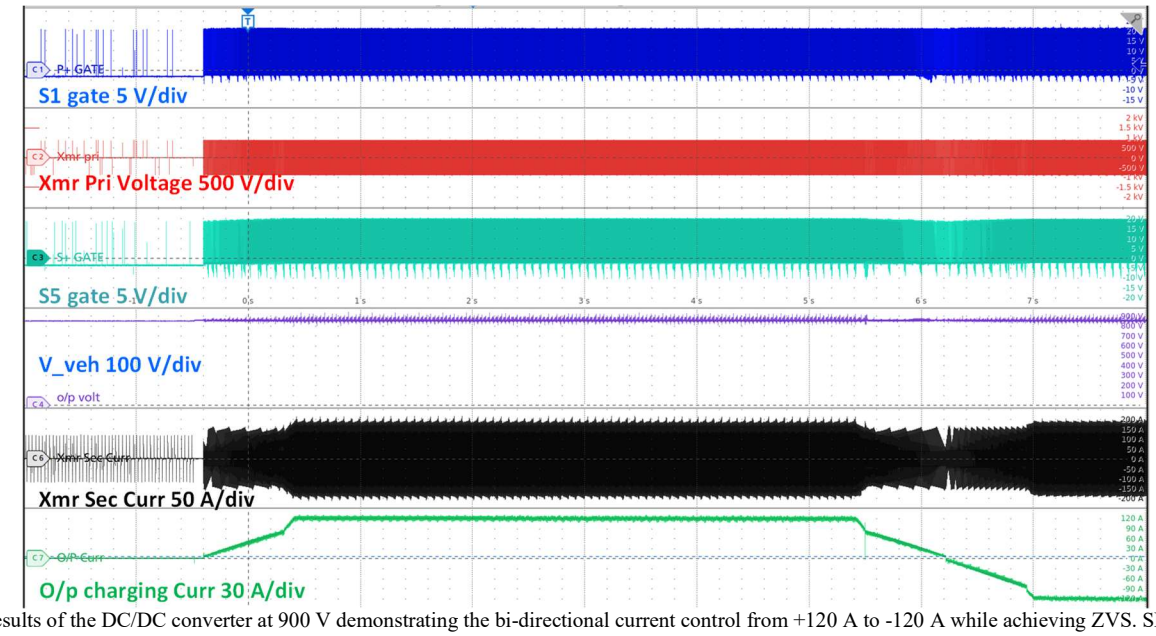

Fig. 9. Results of the DC/DC converter at 900 V demonstrating the bi-directional current control from +120 A to -120 A while achieving ZVS. SPS method is used over |90 A| and proposed ZSM method is used below |90 A|.

secondary is built with a center tap, which is meant for 400 V class vehicles.

TABLE I. DESIGN PARAMETRS AND COMPONENTS FOR THE 950 V 150 A PROTOTYPE

Parameter	***Value***
Bus voltage V_{bus}	900 V nominal, 950 V peak
Vehicle voltage V_{veh}	250 V – 810 V, 580-760 V and 290-380 V for high current
Peak charging current	150 A
Switching frequency F_s	20 kHz
Transformer turns	13/10 (tap at 5)
Magentizing inductance L_m	1.5 mH referred to primary
Effective phase inductance L_{ph}	16 µH referred to secondary
Filter capacitance C	140 µF

B. *Test Conditions*

The converter was tested with input and output buses shorted, for ease of testing. The transformer turns are modified to have an 11/10 turns ratio. Under this scenario, the converter will operate in boost mode for forward power flow and buck mode for reverse flow. Please note that in this test scenario $V_{veh} - V_{bus,sec}$ is 90 V, which is the same as in the regular configuration (760-670 V). Hence the selected configuration tests for the maximum boost/buck voltage range. Simplified ZSM modulation is applied for the test case. As explained in section III b, the timings for ZSM mode for boost mode are derived using the boost model (1)-(7), and values V_{veh}=900 V, $V_{bus,sec}$=810 V, $I_{min} = 40\ A, D_{max} = 23\ \mu s$. The derived timings are shown in Table II. Similarly, the timings for buck derived using (8) –(14) (reverse power low) are also shown. In case of simplified ZSM method, the transition from ZSM to SPS is predetermined and in this case it is 90 A.

TABLE II. TEST CONDITONS FOR THE RESULTS IN THIS PAPER

Parameter	***Value***
Bus voltage V_{bus}	900 V
Vehicle voltage V_{veh}	900 V
Transformer turns	11/10
Devices	1700 V 280 A SiC, MSCSM170AM058CT6LIAG
Magentizing inductance L_m	1.3 mH referred to primary
Effective phase inductance L_{ph}	15 µH referred to secondary
Dead time t_{dead}	600 µH
Min ZVS current I_{min}	40 A for SPS, 50 A for ZSM
t_1, t_3, t_5 and t_z for boost (forward power flow)	3.78 µs, 2 µs, 1.55 µs, 6 µs
t_1, t_3, t_5 and t_z for buck (reverse power flow)	1.55 µs, 2 µs, 3.78 µs, 6 µs
SPS to ZSM transition	90 A

C. *Experimental Results*

The converter is tested to deliver 120 A at 900 V in either direction. The results are shown in Fig. 9. The vehicle voltage V_{veh} is shown in purple, the transformer voltage measured on the primary side is shown in red, the gate voltage for the switch *S1* on the primary bridge is shown in blue, gate voltage for the switch *S5* on the secondary bridge is shown in green, the transformer current measured on the secondary side is shown in black and the output current is shown in green. The output current starts at zero, reaches +120 A, and reverses direction to reach -120 A. The control moves across the following modes: forward-low current mode, forward high current mode, reverse low-current mode, reverse high current mode, and reverse low-current mode. In the low-current modes the converter is operating under ZSM, while in the high current mode standard

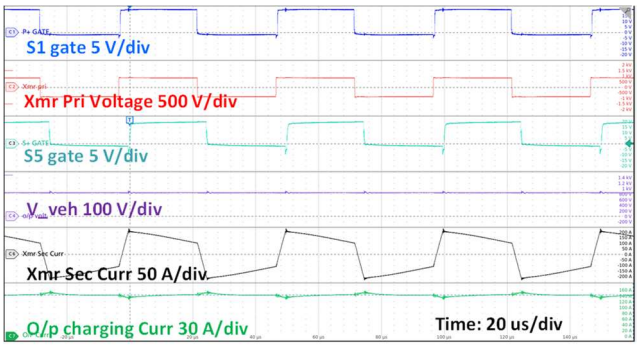

Fig. 10. Results at 900 V 145 A using SPS modulation.

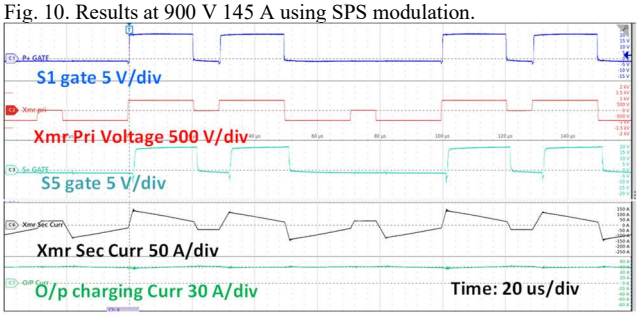

Fig. 11. Results at 900 V 60 A using simplified ZSM modulation.

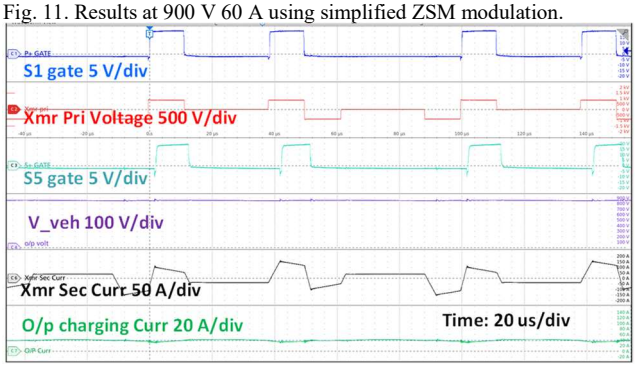

Fig. 12. Results at 900 V 40 A using simplified ZSM modulation.

SPS is used. Transition from low-current to high current modes occur at |90 A| and can be recognized by the change in the ramp rates for the current. The transition between modes does not involve any unwanted transients in the transformer current.

The waveforms for the +145 A operation are shown in Fig. 10. The converter operates in SPS in this high-current mode. The current, shown in black, shows the typical waveform for boost operation in a DAB. The transformer current transitions occur at |I|>40 A, as designed to ensure ZVS.

The zoomed in waveforms for the +60 A and +40 A operation are shown in Fig. 11 and Fig. 12, respectively. At these current levels, simplified ZSM technique is used. The zero state can be identified by the duration where the transformer voltage (in red) is zero. During the zero state, the transformer current is maintained at 40 A as designed. Comparing the transformer current in Fig. 11 and Fig. 12 shows the increased zero state duration in 40 A operation compared to the 60 A operation. This is consistent with the ZSM technique, where the basic idea of current control is through the control of zero state duration. Please note that the transformer current transitions are all at |I|>40 A in both 60 A and 40 A modes, thereby ensuring ZVS turn-on.

The waveforms for +40 A operation using optimal ZSM technique are shown in Fig. 13. Comparing with Fig. 12, where simplified ZSM technique is used, it can be seen that the transformer current has lower peaks and smaller zero state with optimal ZSM technique. This will ensure smaller transformer rms current at the same output current, resulting in higher efficiency.

The waveforms for 60 A in the reverse power flow operation using simplified ZSM technique are shown in Fig. 14. The transformer current shape shows the buck operation. Again the transformer current transitions are all at |I|>40 A, thereby ensuring ZVS turn-on.

The ZVS turn-on behavior is shown in Fig. 15. Intially the transformer current is flowing in S1. After *S1* gate (blue) is turned off, the voltae across *S1* (red) ramps up to the bus voltage. The current is now flowing in the FWD of *S2*. If *S2* is turned on now, it ensure ZVS turn-on. As seen in the figure, the transformer current is still postive (~20 A) at the time of S2 gate (green) beign turned on. The presented current transition is at I_{xmr} = 50 A and the results show a margin of 20 A for ZVS to fail. Based on the observation, it can be assumed that I_{min} = 40

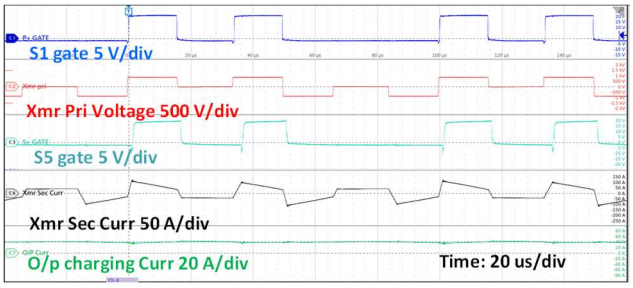

Fig. 13. Results at 900 V 40 A using optimal ZSM modulation.

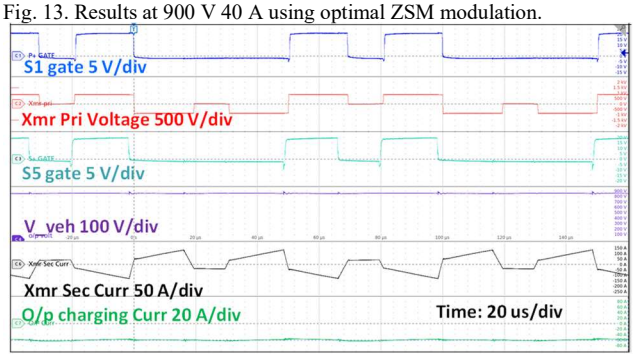

Fig. 14. Results at 900 V -60 A using simplified ZSM modulation demonstrating reverse power flow.

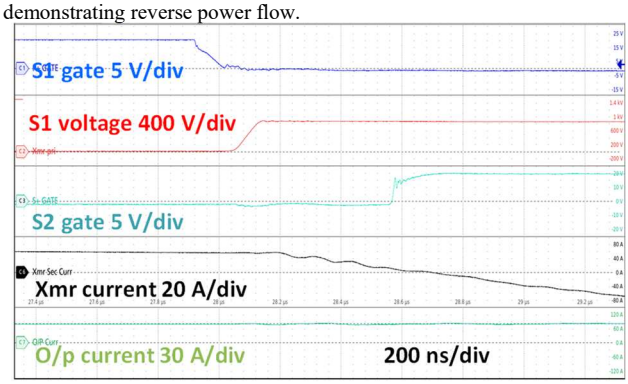

Fig. 15. Zoomed in waveforms to demonstrate ZVS turn-on. S2 gate gets on before transformer current turns negative.

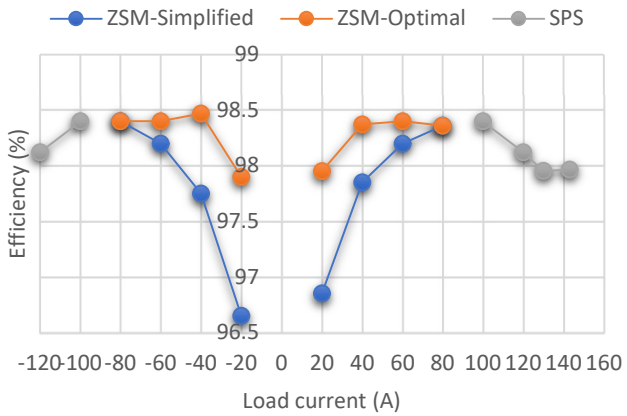

Fig. 16. Measured efficiency at 900 V for different operating modes.

A will ensure ZVS as long as all the current transistions are performed above $|I_{min}|$.

D. *Efficiency Analaysis*

The efficiency of the converter was measured at multiple currents and modes. The results are shown in Fig. 16. In the higher current region, where SPS technique is used, the efficiency is in the range of 98-98.5%. In the lower current region, optimal ZSM and simplifies ZSM technique are compared. The optimal ZSM has 98.5% from 40A-90 A and drops to 98% at 20 A, which is 14% of the nominal current. With the simplified ZSM technique, the efficiency is similar to optimal ZSM at 80 A but decreases at a faster rate to ~97% at 20 A. Since the optimal ZSM optimizes for rms current, in addition to ZVS, the efficiency with the optimal technique is higher compared to the simplified technique and the difference is significant at very low currents. The results show that, with the proposed approach of using ZSM technique at lower currents and SPS at higher currents, it is possible to achieve >98% efficiency from 15%-100% of the nominal current (150 A) while achieving ZVS. The efficiency results presented here are for the highest buck/boost ratio chosen (+/- 15%). The peak efficiency of the converter, which will occur at nominal voltages, is expected to be even higher.

VII. Conclusions

In this paper, the development of a bidirectional DC/DC converter based on DAB for 1 kV class fast charger applications is presented. A novel modulation technique called zero state modulation (ZSM) is proposed to ensure ZVS across the entire voltage and current range of a typical 800 V class vehicle. Model based techniques are used to implement the ZSM technique. Two versions of ZSM technique, optimal and simplified, are proposed. Optimal technique achieves ZVS and minimizes RMS current but need computation for timings (phase shifts) at each switching cycle. Simplifies ZSM method involves predetermined timings (phase shifts), and current control is achieved with only duty cycle variation.

A 1 kV class 150 A DC/DC converter was built to demonstrate the proposed converter implementation. Converter was tested at 900 V 145 A in boost mode (14%), demonstrating ZVS. For the reverse power flow, the converter was tested at 900 V 120 A in buck mode (14%), again demonstrating ZVS. Together the converter demonstrated ~28% voltage control range, while achieving ZVS. A center tap for the transformer is proposed to achieve an additional 28% voltage range around 335 V for the 400 V class vehicle. Converter operation at lower currents (<90A), demonstrating the ability of the proposed ZSM technique to achieve ZVS in both forward and reverse power flow modes, is also presented. Bidirectional current control from +120 A to -120 A was shown to demonstrate smooth transition between ZSM at lower currents and SPS at higher currents.

Peak efficiency of 98.5% was demonstrated at 70% of the nominal load. It was shown that, with the proposed approach of using ZSM technique at lower currents and SPS at higher currents, it is possible to achieve >98% efficiency from 15-100% of the nominal current (150 A), in addition to achieving ZVS. Though not quantified, ZVS operation is expected to improve transformer insulation lifetime and reduce EMI. In summary, the proposed converter implementation allows a full range ZVS bidirectional isolated DC/DC converter, compatible with 400 V and 800 V class vehicles and which delivers >98% efficiency from 15-100% of the nominal load. In this paper, the converter is presented for fast charger applications, however, the it is equally applicable for storage applications and also as an isolated DC/DC stage in MV converters.

Acknowledgment

The authors would like to thank Lee Slezak, Vehicle Systems Manager at DOE Vehicle Technologies Program.

References

[1] Gill, et.al, “Medium Voltage Dual Active Bridge Using 3.3 kV SiC MOSFETs for EV Charging Application”, 2019 IEEE Energy Conversion Congress and Exposition (ECCE), Baltimore, MD, USA.

[2] https://www.energy.gov/femp/bidirectional-charging-and-electric-vehicles-mobile-storage

[3] “Electric vehicle conductive charging system - part 23: Dc electric vehicle charging station,” IEC 61851-23:2014, pp. 1–159, March 2014.

[4] Hao Tu, et. al, “ Extreme Fast Charging of Electric Vehicles: A Technology Overview” IEEE Transaction on Transportation Electrification, 2019.

[5] https://www.pgcconsultancy.com/post/taking-stock-of-sic-part-1-a-review-of-sic-cost-competitiveness-and-a-roadmap-to-lower-costs

[6] Z. Guo, A. Q. Huang, R. E. Hebner, G. C. Montanari and X. Feng, "Characterization of Partial Discharges in High-Frequency Transformer Under PWM Pulses," in IEEE Transactions on Power Electronics, vol. 37, no. 9, pp. 11199-11208, Sept. 2022

[7] Liting Li, et. al, “An Optimized DPS Control for Dual Active Bridge Converters to Secure Full Load Range ZVS with Low Current Stress” IEEE Transaction on Transportation Electrification, 2021.

[8] A Jain, “PWM Control of Dual Active Bridge: Comprehensive Analysis and Experimental Verification,” in IEEE Transactions on Industrial Electronics, VOL. 26, NO. 4, APRIL 2011.

[9] Huang, Y. Wang, Z. Li and W. Lei, "Unified Triple-Phase-Shift Control to Minimize Current Stress and Achieve Full Soft-Switching of Isolated Bidirectional DC–DC Converter," in IEEE Transactions on Industrial Electronics, vol. 63, no. 7, pp. 4169-4179, July 2016.

[10] S. Grzybowski, E.A. Feilat, and P.Knight, „Accelerated Aging Tests on Magnet Wires under High Frequency Pulsating Voltage and High Temperature,” 1999 Conference on Electrical Insulation and Dielectric Phenomena, Austin, TX, USA.

[11] https://www.eesi.org/papers/view/fact-sheet-the-future-of-the-trucking-industry-electric-semi-trucks-2023